

X-ReID: Cross-Instance Transformer for Identity-Level Person Re-Identification

Leqi Shen^{*1,2}, Tao He^{*†1,2}, Yuchen Guo², Guiguang Ding^{†1,2}

¹ School of Software, Tsinghua University, Beijing, China

² Beijing National Research Center for Information Science and Technology (BNRist)
{lunarshen, kevin.92.he, yuchen.w.guo}@gmail.com, dinggg@tsinghua.edu.cn

Abstract

Currently, most existing person re-identification methods use *Instance-Level* features, which are extracted only from a single image. However, these *Instance-Level* features can easily ignore the discriminative information due to the appearance of each identity varies greatly in different images. Thus, it is necessary to exploit *Identity-Level* features, which can be shared across different images of each identity. In this paper, we propose to promote *Instance-Level* features to *Identity-Level* features by employing cross-attention to incorporate information from one image to another of the same identity, thus more unified and discriminative pedestrian information can be obtained. We propose a novel training framework named X-ReID. Specifically, a Cross Intra-Identity Instances module (IntraX) fuses different intra-identity instances to transfer *Identity-Level* knowledge and make *Instance-Level* features more compact. A Cross Inter-Identity Instances module (InterX) involves hard positive and hard negative instances to improve the attention response to the same identity instead of different identity, which minimizes intra-identity variation and maximizes inter-identity variation. Extensive experiments on benchmark datasets show the superiority of our method over existing works. Particularly, on the challenging MSMT17, our proposed method gains 1.1% mAP improvements when compared to the second place.

1 Introduction

Person Re-Identification (ReID) aims to retrieve a person of interest across multiple non-overlapping cameras. Given a single image of an identity, the goal of the ReID model is to learn the pedestrian characteristics, so that the distance of intra-identity features is smaller than that of inter-identity. However, the task of ReID is very challenging, since various complex conditions, such as human pose variations, different backgrounds, or varying illuminations, usually appear on different images of the same identity.

Several previous studies (Ye et al. 2021; Luo et al. 2019b; Chen et al. 2019; Sun et al. 2018; Zhu et al. 2020; He et al. 2021) present promising results on supervised ReID. Since these works extract features from only a single image, rather than from a combination of multiple images of the same identity, we refer to them as *Instance-Level* methods.

^{*}equal contribution

[†]corresponding author

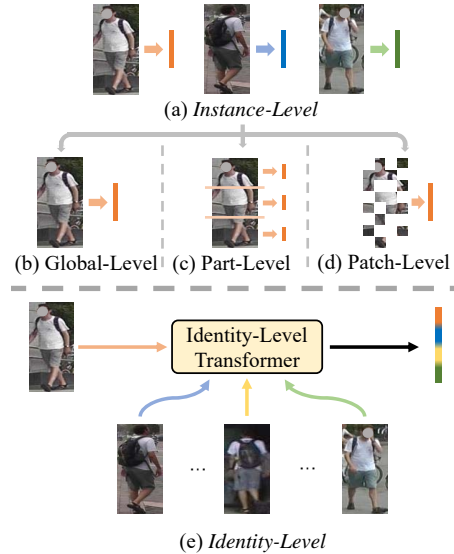


Figure 1: The images on different sides are the same identity. (a) *Instance-Level* methods can be classified into: (b) Global-Level methods, (c) Part-Level methods and (d) Patch-Level methods. As illustrated in (e), our proposed method exploits *Identity-Level* features shared across different images of the same identity.

According to the different processing methods for individual images, *Instance-Level* methods can be roughly classified into the following categories. (1) Global-Level methods (Luo et al. 2019b; Chen et al. 2020, 2019; Zhang et al. 2020; Fang et al. 2019; Si et al. 2018; Zheng et al. 2019; Chen et al. 2018; Luo et al. 2019a), which directly learn the global representation by optimizing *Instance-Level* features of each single complete image, as shown in Figure 1.b. (2) Part-Level methods (Sun et al. 2018; Wang et al. 2018; Li et al. 2021b; Zhu et al. 2020; He and Liu 2020; Zhang et al. 2019; Jin et al. 2020; Zhu et al. 2021, 2022), as shown in Figure 1.c, which learn local aggregated features from different parts. (3) Patch-Level methods such as TransReID (He et al. 2021), which rearranges and re-groups the patch embeddings of each single image (see Figure 1.d). Each group forms an incomplete global representation.

Due to various factors such as human pose and camera variations, the appearance of the same identity varies greatly in different images. Instance-Level methods focus on features only from a single image, so the features of different images of the same identity are prone to large differences. For example, Figure 1.a shows the front and back of the same identity captured by different cameras. As the backpack in the back image is more salient than that in the front image, features independently learned by Instance-Level methods will vary greatly. Consequently, it may lead to intra-identity variation being larger than inter-identity variation, which further limits the performance in inference.

We argue the reason is that Instance-Level methods are unable to learn discriminative features shared across different images of the same identity. To resolve this problem, we propose a novel *Identity-Level* method to fuse different Instance-Level features of the same identity, as shown in Figure 1.e. In this way, more unified and robust pedestrian information can be learned. With our method, for the discriminative information of the “backpack” in the back image, the front can gain knowledge from the back to strengthen its representation, thereby reducing intra-identity variation, enlarging inter-identity variation and obtaining a more robust features.

Our proposed method is based on the pure Transformer structure(Dosovitskiy et al. 2020). The Multi-Head Attention module can exploit long-range dependencies between patches divided from the input image, which can get fine-grained features with rich structural patterns. However, previous works(He et al. 2021; Zhu et al. 2021) only use the Instance-Level Transformer and thus can not jointly encode multiple images to extract Identity-Level features. In this paper, we introduce cross-attention to the encoder, which has not been fully explored in vision task, especially in ReID. Cross-attention can incorporate information from different instances, which mitigates the impact of the variable appearance of the same identity.

Based on the attention mechanism, we introduce a novel training framework, CrossReID termed as X-ReID, which performs attention across different instances of the same identity to extract Identity-Level features. Firstly, we propose a Cross Intra-Identity Instances module (IntraX). Cross-attention is applied among different intra-identity instances to get more unified features. Then, we transfer Identity-Level knowledge to Instance-Level features, which makes features more compact. Second, We further propose a Cross Inter-Identity Instances module (InterX). Hard positive and negative instances are utilized in cross-attention. The fused features, which contain hard negative instance, are less discriminative. The fused features are optimized by our proposed X-Triplet loss to improve the attention response to the same identity rather than different identity, so that intra-identity variation is minimized and inter-identity variation is maximized. Our modules consider both Intra- and Inter-Identity instances to improve the Identity-Level ability of Instance-Level features. Only the improved Instance-Level features are used for inference, which brings no additional cost compared with Transformer-based state-of-the-art methods.

Our major contributions can be summarized as follows:

- We propose to exploit Identity-Level features shared across different images of each identity to build a more unified, discriminative and robust representation.
- We introduce a novel training framework, termed as X-ReID, which contains IntraX for Intra-Identity instances and InterX for Inter-Identity instances to improve the Identity-Level ability of Instance-Level features.
- The overall method is evaluated on benchmark datasets, MSMT17(Wei et al. 2018) and Market1501(Zheng et al. 2015). Extensive experimental results validate the effectiveness of Identity-Level and X-ReID achieves state-of-the-art performance.

2 Related Work

2.1 Supervised ReID

Existing works extract instance representations from a single image, so we refer to them as Instance-Level methods, which can be roughly categorized into three classes: (1) Global-Level methods(Zheng et al. 2017; Luo et al. 2019b), which learn the global representation of each single complete image. The misalignment problem is handled in attention-based methods(Chen et al. 2020, 2019; Zhang et al. 2020; Fang et al. 2019; Si et al. 2018; Zheng et al. 2019; Chen et al. 2018; Luo et al. 2019a). (2) Part-Level methods(Sun et al. 2018; Wang et al. 2018; Li et al. 2021b; Zhu et al. 2020; He and Liu 2020; Zhang et al. 2019; Jin et al. 2020; Zhu et al. 2021), which learn local aggregated features from different parts. (3) Patch-Level methods such as TransReID(He et al. 2021), which shuffles patches into several incomplete representations.

There are a few CNN-based works that leverage the cross-image information. These works mine the relationships between multiple Instance-Level feature maps. DuATM(Si et al. 2018) performs dually attentive comparison for pairwise feature alignment and refinement. CASN(Zheng et al. 2019) designs a Siamese network with attention consistency. Group similarity is proposed in GCSL(Chen et al. 2018) for learning robust multi-scale local similarities. SFT(Luo et al. 2019a) optimizes group-wise similarities to capture potential relational structure.

2.2 Transformer in Vision

Inspired by the success of Transformers(Vaswani et al. 2017) in natural language tasks, many studies(Khan et al. 2021; Han et al. 2020; Gao et al. 2021; Carion et al. 2020; Xie et al. 2021; Zhao et al. 2021; Chen et al. 2021) have shown the superiority of Transformer in vision tasks. ViT(Dosovitskiy et al. 2020) first introduces a pure Transformer to image classification.

In the field of ReID, PAT(Li et al. 2021b) utilizes Transformer to improve CNN backbone(He et al. 2016). NFormer(Wang et al. 2022) proposes a parametric post-processing method by modeling the relations among all the input images. TransReID(He et al. 2021) investigates a pure Transformer encoder framework, and AAformer(Zhu et al. 2021) integrates the part alignment into the self-attention.

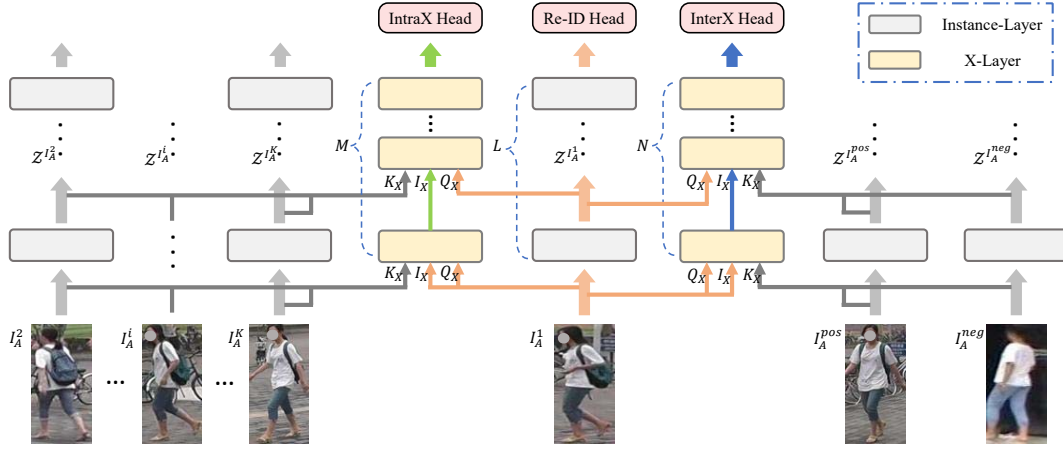


Figure 2: Framework of our proposed X-ReID, based on L layers Instance-Level Transformer. It is composed of a Cross Intra-Identity Instances module (IntraX) and a Cross Inter-Identity Instances (InterX). We build M X-Layers for IntraX, N X-Layers for InterX, and set $M = N = L$. The details of X-Layer are shown in Figure 4.

DCAL(Zhu et al. 2022) introduces cross-attention mechanisms to learn subtle feature embeddings. Instead, we exploit cross-attention to fuse Instance-Level features.

As for image classification, cross-attention in CrossViT(Chen, Fan, and Panda 2021) is used to learn multi-scale features. In Trear(Li et al. 2021a), features from different modalities are fused to obtain the conjoint cross-modal representation. Unlike these approaches, our proposed cross-attention extracts Identity-Level features for more unified and discriminative pedestrian information.

3 Method

Our method is built on top of pure Transformer architecture, so we first present a brief overview of Instance-Level Transformer in Sec 3.1. Then, we introduce the proposed Identity-Level framework (X-ReID) in Sec 3.2, which contains a Cross Intra-Identity Instances module (IntraX) and a Cross Inter-Identity Instances (InterX).

3.1 Instance-Level Transformer for ReID

Instance-Level Transformer for ReID is a Transformer-based strong baseline and we follow the baseline in TransReID(He et al. 2021). As shown in Figure 3, given a single input image, we reshape it into a sequence of flattened patches $N \times (P^2 \times C)$, where C is the number of channels. P is the resolution of each patch, and N is the length of fixed-sized patches according to image size. We flatten the patches and map to vectors with a trainable linear projection. An extra learnable embedding CLS is added to the sequence of embedded patches. Learnable position embeddings are used for retaining spatial information. The output embeddings can be expressed as: $\mathcal{Z}_0 = [z_{cls}^0; z_1^0; \dots; z_N^0]$, where \mathcal{Z}_0 represents the input fed into backbone, z_{cls} is CLS token and $z_{patch} = \{z_i | i = 1, \dots, N\}$ are patch tokens.

The backbone is composed of a stack of L identical Transformer layers. Because the input is a single image and the layers encode the Instance-Level information, the Trans-

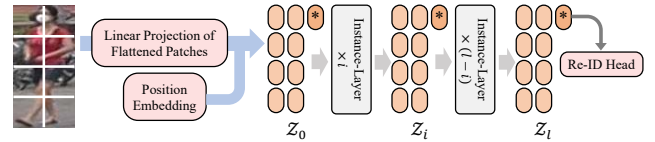


Figure 3: Framework of Instance-Level Transformer. * refers to CLS token.

former layer is named as Instance-Layer in this paper. And each layer can encode the embeddings: $\mathcal{Z}_i = f(\mathcal{Z}_{i-1} | \theta_{In_s}^i)$, where \mathcal{Z}_i is the output of the i -th Instance-Layer and $\theta_{In_s}^i$ is the weight of this layer. After LayerNorm(Ba, Kiros, and Hinton 2016), the last layer's output of CLS token z_{cls}^L gets Instance-Level features f_{In_s} , to extract global representation, which is used to calculate ID loss(Zheng, Zheng, and Yang 2017) \mathcal{L}_{ID} and Triplet loss(Liu et al. 2017) \mathcal{L}_{Tri} that constitute the ReID Head(Luo et al. 2019b):

$$\mathcal{L}_{In_s} = \mathcal{L}_{ID}(f_{In_s}) + \mathcal{L}_{Tri}(f_{In_s}) \quad (1)$$

3.2 X-ReID

Our proposed Identity-Level framework is illustrated in Figure 2 based on Instance-Level Transformer, which contains IntraX and InterX. For a single image I_A^1 of person A , the tokens obtained from Instance-Level Transformer are $\mathcal{Z}^{I_A^1} = \{\mathcal{Z}_i^{I_A^1} | i = 0, 1, \dots, L\}$. On the left side of Figure 2, as for other images of the same person A , we get $\{\mathcal{Z}^{I_A^i} | i = 2, \dots, K\}$. IntraX are performed among Intra-Identity instances. $\{\mathcal{Z}^{I_A^i}\}$ as Key and $\mathcal{Z}^{I_A^1}$ as Query are fed to X-Layers to extract Identity-Level features f_{IntraX} of person A . Rather than all positive instances as IntraX does, InterX utilizes both positive instance I_A^{pos} and negative instance I_A^{neg} . As shown on the right side of Figure 2, $\mathcal{Z}^{I_A^{pos}}$ and $\mathcal{Z}^{I_A^{neg}}$ are used as Key and we get features f_{InterX} . Our

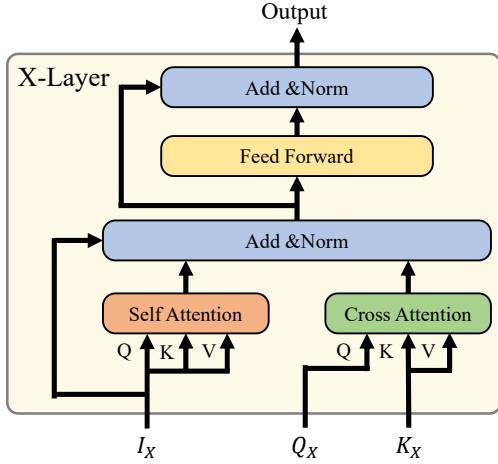


Figure 4: Illustration of X-Layer. In both IntraX and InterX, Q_X are the same. In IntraX, K_X are all positive instances in the mini-batch. As for InterX, K_X are hard positive and hard negative. I_X are usually the output of the previous Layer.

X-ReID explores both Intra- and Inter-Identity instances to enhance Instance-Level features.

X-Layer. Instance-Layer, which consists of alternating layers of **Multi-Head Attention** and FFN blocks, only has Self Attention. The output of MHA is formulated as:

$$\text{MHA}(Q, K, V) = \text{softmax}\left(\frac{QK^T}{\sqrt{d_k}}\right)V \quad (2)$$

where d_k is the scaling factor. Figure 4 shows the detailed structure of our proposed X-Layer. Cross Attention is added to Instance-Layer to become X-Layer. With Cross Attention, X-Layer can obtain features across multiple inputs:

$$\text{Attention}_X(I_X, Q_X, K_X) = \text{MHA}(I_X, I_X, I_X) + \text{MHA}(Q_X, K_X, K_X) \quad (3)$$

where $\text{MHA}(I_X, I_X, I_X)$ is Self Attention and $\text{MHA}(Q_X, K_X, K_X)$ is Cross Attention. It is worth noting that Self Attention and Cross Attention share parameters, so the parameters of X-Layer are the same as those of Instance-Layer.

Cross Intra-Identity Instances. We propose a Cross Intra-Identity Instances module to transfer Identity-Level knowledge to Instance-Level features. All positive instances of the input I_A^1 are fused in X-Layer to extract Identity-Level features. To enhance the Identity-Level capability, IntraX trains Instance-Level features to predict Identity-Level representation of the same identity by knowledge distillation.

M layers of X-Layer in IntraX uses the **Exponential Moving Average (EMA)** on Instance-Layers, which is proposed to maintain consistency. Specifically, the parameters of i -th X-Layer can be calculated as:

$$\theta_{\text{IntraX}}^i \leftarrow \lambda \times \theta_{\text{IntraX}}^i + (1 - \lambda) \times \theta_{\text{Ins}}^i \quad (4)$$

where λ follows a cosine schedule from 0.999 to 1 during training. Knowledge about the different appearances of person A is mixed in X-Layer. I_X , Q_X and K_X of i -th X-Layer in IntraX are:

$$\begin{aligned} I_X^i &= \text{Attention}_X(I_X^{i-1}, Q_X^{i-1}, K_X^{i-1}) \\ Q_X^i &= \mathcal{Z}_i^{I_A^1}, K_X^i = [\mathcal{Z}_i^{I_A^2} || \dots || \mathcal{Z}_i^{I_A^K}] \end{aligned} \quad (5)$$

where I_X^{i-1} are the outputs of the previous X-Layer, except that I_X of the first layer are the same as $Q_x = \mathcal{Z}_0^{I_A^1}$. We concatenates all features of positive instances of I_A^1 in the mini-batch to get $K_X \in \mathbb{R}^{(K-1)C}$. On account of X-Layer, IntraX incorporates different appearances of the same identity into Identity-Level features f_{IntraX} . Then, we transfer the knowledge from f_{IntraX} to f_{Ins} :

$$P(f)^{(i)} = \frac{\exp(f^{(i)}/\tau)}{\sum_{d=1}^C \exp(f^{(d)}/\tau)} \quad (6)$$

$$\mathcal{L}_{\text{IntraX}} = -\sum_{d=1}^C P(f_{\text{IntraX}})^{(d)} \log P(f_{\text{Ins}})^{(d)}$$

where $C = 768$ are the dimensions of features and $\tau = 0.05$ is a temperature parameter. The output of a softmax of the dot products of f is the probability distribution P , which provides information on how the features represent knowledge. Matching distributions of f_{Ins} and f_{IntraX} by minimizing $\mathcal{L}_{\text{IntraX}}$ is used to improve Instance-Level features by Identity-Level features. Therefore, Instance-Level features are more compact.

Cross Inter-Identity Instances. Our proposed Cross Inter-Identity Instances module deals with inter-identity instances of I_A^1 , instead of all positive instances in IntraX. InterX uses both hard positive and hard negative as K_X of X-Layer, where the negative instance I_A^{neg} has not the same identity as the anchor I_A^1 . X-Layers in InterX may incorrectly notice the negative, whose interfering information affects the final fused features of InterX. We optimize the fused features to suppress the attention response of the anchor to negative instance and improve the attention response to positive instance, so that intra-identity variation is minimized and inter-identity variation is maximized.

Particularly, InterX contains N layers of X-Layer that are learnable. I_X and Q_X are the same as in Equation 5. K_X of i -th X-Layer in interX is:

$$K_X^i = [\mathcal{Z}_i^{I_A^{\text{pos}}} || \mathcal{Z}_i^{I_A^{\text{neg}}}] \quad (7)$$

where K_X^i is the result of concatenating $\mathcal{Z}_i^{I_A^{\text{pos}}}$ of hard positive I_A^{pos} and $\mathcal{Z}_i^{I_A^{\text{neg}}}$ of hard negative I_A^{neg} . We conduct hard-mining(Hermans, Beyer, and Leibe 2017) in \mathcal{L}_{Tri} to get hard positive and negative instance. As illustrated in Figure 5.a, \mathcal{L}_{Tri} in the ReID Head is calculated as follows:

$$\mathcal{L}_{\text{Tri}}(a, p, n) = \log[1 + \exp(\|f_a - f_p\|_2^2 - \|f_a - f_n\|_2^2)] \quad (8)$$

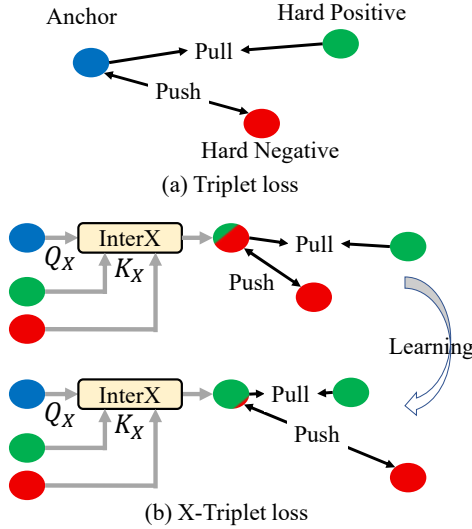


Figure 5: (a) Hard-mining in Triplet loss selects the hardest positive and the hardest negative instances within the batch. (b) X-Triplet loss optimize the fused features from hard positive and negative. Hard positive will have more attention responses than hard negative in X-Layer.

where a , p and n is the anchor, hard positive and hard negative. The anchor may be closer to hard negative compared to hard positive. Therefore in Figure 5.b, the anchor as Q_X is difficult to distinguish which one is positive in InterX. The fused features will be heavily influenced by hard negative. Red represents hard negative and green represents hard positive. In the fused features f_{InterX} , red occupies most of the space. Then, we propose X-Triplet loss:

$$\mathcal{L}_{XTri}(f_{InterX}) = L_{Tri}(f_{InterX}, p, n) \quad (9)$$

Therefore, f_{InterX} is pulled into hard positive and pushed away by hard negative. Then, the InterX Head composed of \mathcal{L}_{ID} and \mathcal{L}_{XTri} are shown as follows:

$$\mathcal{L}_{InterX} = L_{ID}(f_{InterX}) + L_{XTri}(f_{InterX}) \quad (10)$$

By \mathcal{L}_{InterX} , the anchor are encouraged to pay more attention to hard positive than hard negative in X-Layer. f_{InterX} will be optimized to represent the person of the anchor and hard positive. At this stage, green occupies most of the space. Accordingly, InterX simultaneously reduces the distance of intra-identity and enlarges the distance of inter-identity.

Loss Function. In the training phase, the overall objective function is:

$$\mathcal{L}_{X-ReID} = \mathcal{L}_{Ins} + \lambda_1 \mathcal{L}_{IntraX} + \lambda_2 \mathcal{L}_{InterX} \quad (11)$$

where λ_1 and λ_2 are hyper-parameters to balance the entire loss. Notably, only the boosted Instance-Level features f_{Ins} is used for inference. In this way, the final model has the same structure as Instance-Level Transformer whose input is a single image.

4 Experiments

4.1 Evaluation Setting and Metrics

Our proposed method are evaluated on the popular benchmark datasets: MSMT-17(Wei et al. 2018) which contains 126441 person images of 4101 identities, Market1501(Zheng et al. 2015) which contains 32668 person images of 1501 identities. Following the common setting, the cumulative matching characteristics (CMC) at Rank-1 and the mean average precision (mAP) are adopted to evaluate the performance of all methods.

4.2 Implementation Details

We use the ImageNet(Deng et al. 2009)-pretrained model of ViT-Base, which contains $L = 12$ Instance-Layers and the patch size is 16×16 . We build $M = N = 12$ X-Layers in both IntraX and InterX. X-Layers in IntraX use an exponential moving average on Instance-Layer. X-layers are learnable in InterX. In Equation 11, we set $\lambda_1 = 5.0, \lambda_2 = 0.4$ and $\lambda_1 = 20.0, \lambda_2 = 0.4$ for Market1501 and MSMT17, respectively. The input images are resized to 256×128 . Following common practices, random horizontal flipping, padding, random cropping and random erasing(Zhong et al. 2020) are used as augmentation for training. We randomly sample $K = 4$ instances for each identity in a mini-batch with batch size 64. SGD optimizer with a momentum of 0.9 and the weight decay of $1e-4$ is applied with a learning rate of 0.008 with cosine learning rate decay. We train 120 epochs in total. All the experiments are performed with one NVIDIA Geforce RTX 3090.

4.3 Comparisons with State-of-the-art Methods

In Table 1, we compare our proposed X-ReID with state-of-the-art methods on MSMT17 and Market1501. On Market1501, our method achieves comparable performance with the recent Transformer-based methods, especially on mAP. On the challenging MSMT17, Transformer-based methods outperform CNN-based methods significantly. X-ReID reaches state-of-the-art performance, which gains 1.1% mAP improvements when compared to the second place.

Our Baseline follows the setup in (He et al. 2021). The Baselines of X-ReID and TransReID have the same implementation. In order to compare the experiments better, we reproduce Baseline and TransReID, whose performance is slightly different from that in the original paper due to different hardware environments. Our X-ReID is the Baseline with proposed IntraX and InterX. Based on the same Baseline, X-ReID outperforms TransReID by 1.6% mAP on MSMT17 and 0.6% mAP on Market1501.

CNN-based methods in the 1st group leverage the cross-image information, which mine the relations among Instance-Level features. Transformer-based DCAL(Zhu et al. 2022) proposes cross-attention to learn local features better, which is classified as a Part-Level method. However, our proposed Identity-Level method are introduced to extract more unified features among all intra-identity instances and push inter-identity instances far away. X-ReID surpasses the CNN-based cross-image methods by a large margin, at least 5.3% mAP on Market1501. X-ReID outperforms

Table 1: Comparison with state-of-the-art training methods. * means we re-implement the experiments based on the official code. Baseline* is Instance-Level Transformer described in Sec 3.1, which follows the setup in (He et al. 2021). TransReID* is the result without side information for fair comparison.

Backbone	Methods	Ref	MSMT17		Market1501	
			mAP	Rank-1	mAP	Rank-1
CNN	DuATM(Si et al. 2018)	CVPR2018	-	-	76.6	91.4
	GCSL(Chen et al. 2018)	CVPR2018	-	-	81.6	93.5
	CASN(Zheng et al. 2019)	CVPR2019	-	-	82.8	94.4
	SFT(Luo et al. 2019a)	ICCV2019	47.6	73.6	82.7	93.4
	PAT(Li et al. 2021b)	CVPR2021	-	-	88.0	95.4
	ISP(Zhu et al. 2020)	ECCV2020	-	-	88.6	95.3
	PCB(Sun et al. 2018)	ECCV2018	40.4	68.2	81.6	93.8
	SCSN(Chen et al. 2020)	CVPR2020	58.5	83.8	88.5	95.7
	ABDNet(Chen et al. 2019)	ICCV2019	60.8	82.3	88.3	95.6
Transformer	Baseline*(He et al. 2021)	ICCV2021	62.3	82.2	87.1	94.6
	AAformer(Zhu et al. 2021)	Arxiv2021	63.2	83.6	87.7	95.2
	TransReID*(He et al. 2021)	ICCV2021	63.5	83.0	87.4	94.2
	DCAL(Zhu et al. 2022)	CVPR2022	64.0	83.1	87.5	94.7
	X-ReID	Ours	65.1	84.0	88.0	94.9

the cross-attention related method DCAL by 1.1% mAP on MSMT17 and 0.5% mAP on Market1501.

4.4 Effectiveness of X-ReID

We propose to improve Instance-Level features with our Identity-Level framework. Compared to Instance-Level features generated from a single image, Identity-Level features, generated across different images of each identity, have more unified pedestrian information. So that in X-ReID, different Instance-Level features of each identity are very compact and features from different identities are easy to distinguish, which facilitates the model to learn more discriminative and unified features.

Compactness Analysis. We evaluate intra-identity variation as follows:

$$\omega_i = \frac{1}{|\Omega_i|} \sum_{x_j \in \Omega_i} x_j, CP_i = \frac{1}{|\Omega_i|} \sum_{x_j \in \Omega_i} \|x_j - \omega_i\|$$

$$CP = \frac{1}{N} \sum_{k=1}^N CP_k \quad (12)$$

where Ω_i denotes the set containing all the feature vectors of the i -th person and ω_i represents the feature center of the i -th person. CP_i calculates the average distance from each instance to the center in the i -th person. N is the number of persons and the overall compactness CP is the mean compactness of all persons. The lower the value of CP , the more compact the features of each identity. Figure 6 shows the compactness of different persons in the test set on MSMT17 and Market1501. Although TransReID outperforms Baseline, the compactness is almost the same. With Identity-Level, the compactness is much lower than Baseline and TransReID. Such results prove the Identity-Level knowledge can reduce intra-identity variation.

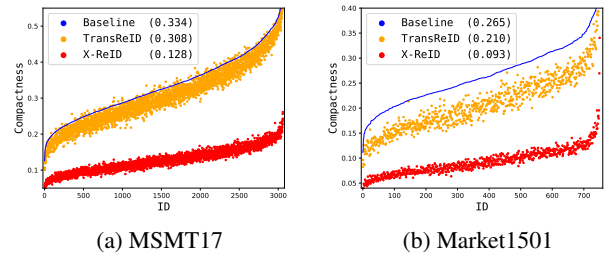


Figure 6: Compactness analysis in the test set on MSMT17 and Market1501. The order of the person ID axis is in ascending order of the compactness of Baseline. The overall compactness is shown in the parentheses.

The Calinski-Harabasz Score Analysis. The Calinski-Harabasz score (Caliński and Harabasz 1974) is defined as ratio of the sum of between-cluster dispersion and of within-cluster dispersion, which can be used to evaluate intra- and inter-identity variations. CH is higher when identities are both dense and well separated. Fig.7 shows CH metric during the training epochs. We can find that the curves of TransReID and Baseline rise slowly and the curve of X-ReID rises rapidly. The curve of X-ReID is significantly higher than that of TransReID and Baseline. By our proposed method, intra-identity instances are more compact and inter-identity instances are well separated.

Visualization Analysis. In Figure 8, we further conduct visualization experiments(Chefer, Gur, and Wolf 2021) to show the effectiveness of X-ReID. We compare our method with Baseline and TransReID. Our model focuses on more comprehensive areas, while high attention regions are relatively scattered instead of focusing on a small area, which indicates that our model can obtain more unified pedestrian

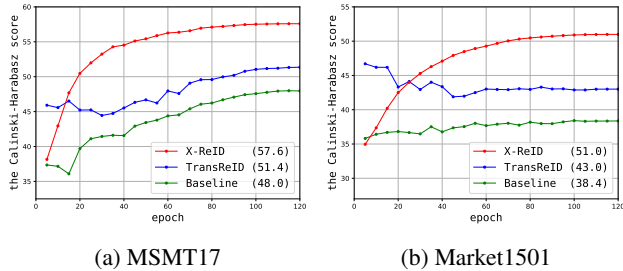


Figure 7: The Calinski-Harabasz score analysis in the test set on MSMT17 and Market1501. CH is calculated every 5 training epochs. The value in the parentheses is CH of the final model.

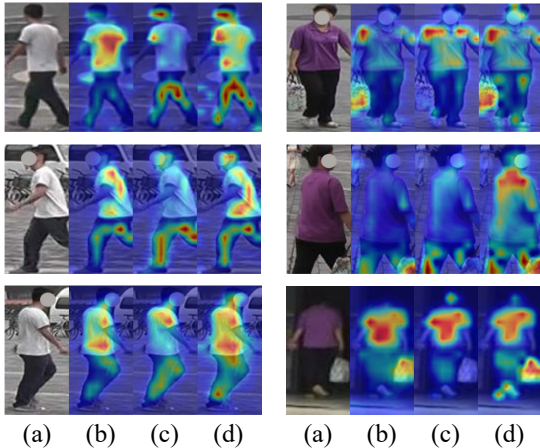


Figure 8: Visualization analysis of attention maps. (a) Input images, (b) Baseline, (c) TransReID, (d) X-ReID. The images in each column are the same identity.

information. In the second column, the “handbag” is only a small part of the middle image. Our model learns the Identity-Level information from multiple images to improve the discriminative ability to recognize the “handbag”.

4.5 Ablation Studies of X-ReID

The effectiveness of individual components. There are two important components in our proposed X-ReID: a Cross Intra-Identity Instances module (IntraX) and a Cross Inter-Identity Instances module (InterX). We evaluate the contribution of each component in Table 2. EMA means the Exponential Moving Average operation in IntraX. The improvement of Baseline+IntraX is more impressive than that of Baseline+EMA, which validates the effectiveness of Identity-Level rather than EMA. Through fusing intra-identity instances, IntraX transfer the Identity-Level knowledge to Instance-Level features to gain promising performance. InterX deals with inter-identity instances to minimize intra-identity variation and maximize inter-identity variation. Compared with Baseline, our full X-ReID significantly boosts the performance by 2.8% mAP and 0.9% mAP on MSMT17 and Market1501, respectively.

Table 2: The ablation study on individual components of X-ReID. EMA is IntraX without \mathcal{L}_{IntraX} .

Methods	MSMT17		Market1501	
	mAP	Rank-1	mAP	Rank-1
Baseline	62.3	82.2	87.1	94.6
Baseline+EMA	62.4	82.3	87.1	94.7
Baseline+IntraX	64.7	83.4	87.8	94.7
Baseline+InterX	63.7	83.2	87.4	94.7
X-ReID	65.1	84.0	88.0	94.9

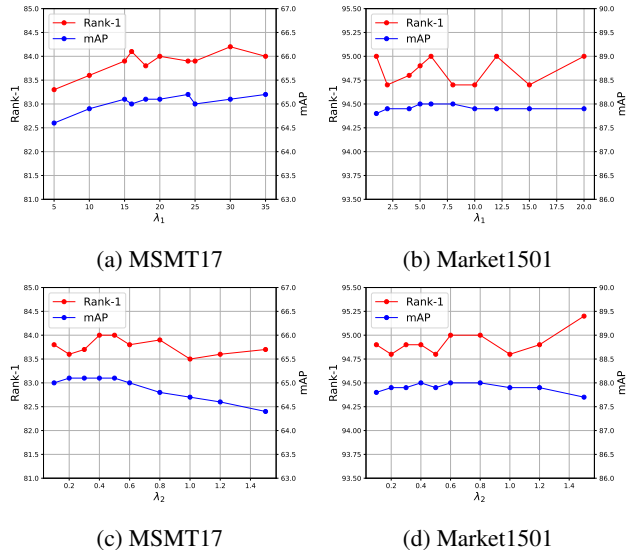


Figure 9: Hyper-parameters analysis of weight λ_1 and λ_2 of the entire loss on MSMT17 and Market1501.

Hyper-parameters Analysis We evaluate the impact of weight λ_1 and λ_2 of the entire loss (Equation 11) in Figure 9. λ_1 balances the weight of IntraX and λ_2 balances the weight of InterX. The first row shows the impact of λ_1 when λ_2 is fixed at 0.4. Although the final selected λ_1 is not the same on the two datasets, the performance fluctuates very little with the change of λ_1 and mAP is at least above 64.6% on MSMT17. The second row shows the impact of λ_2 when λ_1 is fixed at 20.0 on MSMT17 and 5.0 on Market1501. The performance obtains a further improvement when the value of λ_2 is around 0.4.

5 Conclusion and Future Work

In this paper, we propose a novel training framework named X-ReID, which contains a Cross Intra-Identity Instances module and a Cross Inter-Identity Instances module. Our proposed methods extract Identity-Level features for more unified and discriminative pedestrian information. Extensive experiments on benchmark datasets show the superiority of our methods over state-of-the-art methods. In the future, more sophisticated solutions for improving the Identity-Level capability can be exploited.

References

- Ba, J. L.; Kiros, J. R.; and Hinton, G. E. 2016. Layer normalization. *arXiv preprint arXiv:1607.06450*.
- Caliński, T.; and Harabasz, J. 1974. A dendrite method for cluster analysis. *Communications in Statistics-theory and Methods*, 3(1): 1–27.
- Carion, N.; Massa, F.; Synnaeve, G.; Usunier, N.; Kirillov, A.; and Zagoruyko, S. 2020. End-to-end object detection with transformers. In *European conference on computer vision*, 213–229. Springer.
- Chefer, H.; Gur, S.; and Wolf, L. 2021. Transformer interpretability beyond attention visualization. In *Proceedings of the IEEE/CVF Conference on Computer Vision and Pattern Recognition*, 782–791.
- Chen, C.-F. R.; Fan, Q.; and Panda, R. 2021. Crossvit: Cross-attention multi-scale vision transformer for image classification. In *Proceedings of the IEEE/CVF International Conference on Computer Vision*, 357–366.
- Chen, D.; Xu, D.; Li, H.; Sebe, N.; and Wang, X. 2018. Group consistent similarity learning via deep crf for person re-identification. In *Proceedings of the IEEE conference on computer vision and pattern recognition*, 8649–8658.
- Chen, H.; Wang, Y.; Guo, T.; Xu, C.; Deng, Y.; Liu, Z.; Ma, S.; Xu, C.; Xu, C.; and Gao, W. 2021. Pre-trained image processing transformer. In *Proceedings of the IEEE/CVF Conference on Computer Vision and Pattern Recognition*, 12299–12310.
- Chen, T.; Ding, S.; Xie, J.; Yuan, Y.; Chen, W.; Yang, Y.; Ren, Z.; and Wang, Z. 2019. Abd-net: Attentive but diverse person re-identification. In *Proceedings of the IEEE/CVF International Conference on Computer Vision*, 8351–8361.
- Chen, X.; Fu, C.; Zhao, Y.; Zheng, F.; Song, J.; Ji, R.; and Yang, Y. 2020. Saliency-guided cascaded suppression network for person re-identification. In *Proceedings of the IEEE/CVF Conference on Computer Vision and Pattern Recognition*, 3300–3310.
- Deng, J.; Dong, W.; Socher, R.; Li, L.-J.; Li, K.; and Fei-Fei, L. 2009. Imagenet: A large-scale hierarchical image database. In *2009 IEEE conference on computer vision and pattern recognition*, 248–255. Ieee.
- Dosovitskiy, A.; Beyer, L.; Kolesnikov, A.; Weissenborn, D.; Zhai, X.; Unterthiner, T.; Dehghani, M.; Minderer, M.; Heigold, G.; Gelly, S.; et al. 2020. An image is worth 16x16 words: Transformers for image recognition at scale. *arXiv preprint arXiv:2010.11929*.
- Fang, P.; Zhou, J.; Roy, S. K.; Petersson, L.; and Harandi, M. 2019. Bilinear attention networks for person retrieval. In *Proceedings of the IEEE/CVF international conference on computer vision*, 8030–8039.
- Gao, W.; Wan, F.; Pan, X.; Peng, Z.; Tian, Q.; Han, Z.; Zhou, B.; and Ye, Q. 2021. TS-CAM: Token Semantic Coupled Attention Map for Weakly Supervised Object Localization. In *Proceedings of the IEEE/CVF International Conference on Computer Vision*, 2886–2895.
- Han, K.; Wang, Y.; Chen, H.; Chen, X.; Guo, J.; Liu, Z.; Tang, Y.; Xiao, A.; Xu, C.; Xu, Y.; et al. 2020. A survey on visual transformer. *arXiv e-prints*, arXiv–2012.
- He, K.; Zhang, X.; Ren, S.; and Sun, J. 2016. Deep residual learning for image recognition. In *Proceedings of the IEEE conference on computer vision and pattern recognition*, 770–778.
- He, L.; and Liu, W. 2020. Guided saliency feature learning for person re-identification in crowded scenes. In *European Conference on Computer Vision*, 357–373. Springer.
- He, S.; Luo, H.; Wang, P.; Wang, F.; Li, H.; and Jiang, W. 2021. Transreid: Transformer-based object re-identification. In *Proceedings of the IEEE/CVF International Conference on Computer Vision*, 15013–15022.
- Hermans, A.; Beyer, L.; and Leibe, B. 2017. In defense of the triplet loss for person re-identification. *arXiv preprint arXiv:1703.07737*.
- Jin, X.; Lan, C.; Zeng, W.; Wei, G.; and Chen, Z. 2020. Semantics-aligned representation learning for person re-identification. In *Proceedings of the AAAI Conference on Artificial Intelligence*, volume 34, 11173–11180.
- Khan, S.; Naseer, M.; Hayat, M.; Zamir, S. W.; Khan, F. S.; and Shah, M. 2021. Transformers in vision: A survey. *ACM Computing Surveys (CSUR)*.
- Li, X.; Hou, Y.; Wang, P.; Gao, Z.; Xu, M.; and Li, W. 2021a. Trear: Transformer-based rgb-d egocentric action recognition. *IEEE Transactions on Cognitive and Developmental Systems*.
- Li, Y.; He, J.; Zhang, T.; Liu, X.; Zhang, Y.; and Wu, F. 2021b. Diverse part discovery: Occluded person re-identification with part-aware transformer. In *Proceedings of the IEEE/CVF Conference on Computer Vision and Pattern Recognition*, 2898–2907.
- Liu, H.; Feng, J.; Qi, M.; Jiang, J.; and Yan, S. 2017. End-to-end comparative attention networks for person re-identification. *IEEE Transactions on Image Processing*, 26(7): 3492–3506.
- Luo, C.; Chen, Y.; Wang, N.; and Zhang, Z. 2019a. Spectral feature transformation for person re-identification. In *Proceedings of the IEEE/CVF International Conference on Computer Vision*, 4976–4985.
- Luo, H.; Gu, Y.; Liao, X.; Lai, S.; and Jiang, W. 2019b. Bag of tricks and a strong baseline for deep person re-identification. In *Proceedings of the IEEE/CVF conference on computer vision and pattern recognition workshops*, 0–0.
- Si, J.; Zhang, H.; Li, C.-G.; Kuen, J.; Kong, X.; Kot, A. C.; and Wang, G. 2018. Dual attention matching network for context-aware feature sequence based person re-identification. In *Proceedings of the IEEE conference on computer vision and pattern recognition*, 5363–5372.
- Sun, Y.; Zheng, L.; Yang, Y.; Tian, Q.; and Wang, S. 2018. Beyond part models: Person retrieval with refined part pooling (and a strong convolutional baseline). In *Proceedings of the European conference on computer vision*, 480–496.
- Vaswani, A.; Shazeer, N.; Parmar, N.; Uszkoreit, J.; Jones, L.; Gomez, A. N.; Kaiser, Ł.; and Polosukhin, I. 2017. Attention is all you need. *Advances in neural information processing systems*, 30.

- Wang, G.; Yuan, Y.; Chen, X.; Li, J.; and Zhou, X. 2018. Learning discriminative features with multiple granularities for person re-identification. In *Proceedings of the 26th ACM international conference on Multimedia*, 274–282.
- Wang, H.; Shen, J.; Liu, Y.; Gao, Y.; and Gavves, E. 2022. NFormer: Robust Person Re-identification with Neighbor Transformer. In *Proceedings of the IEEE/CVF Conference on Computer Vision and Pattern Recognition*, 7297–7307.
- Wei, L.; Zhang, S.; Gao, W.; and Tian, Q. 2018. Person transfer gan to bridge domain gap for person re-identification. In *Proceedings of the IEEE conference on computer vision and pattern recognition*, 79–88.
- Xie, E.; Wang, W.; Yu, Z.; Anandkumar, A.; Alvarez, J. M.; and Luo, P. 2021. SegFormer: Simple and efficient design for semantic segmentation with transformers. *Advances in Neural Information Processing Systems*, 34.
- Ye, M.; Shen, J.; Lin, G.; Xiang, T.; Shao, L.; and Hoi, S. C. 2021. Deep learning for person re-identification: A survey and outlook. *IEEE Transactions on Pattern Analysis and Machine Intelligence*.
- Zhang, Z.; Lan, C.; Zeng, W.; and Chen, Z. 2019. Densely semantically aligned person re-identification. In *Proceedings of the IEEE/CVF Conference on Computer Vision and Pattern Recognition*, 667–676.
- Zhang, Z.; Lan, C.; Zeng, W.; Jin, X.; and Chen, Z. 2020. Relation-aware global attention for person re-identification. In *Proceedings of the IEEE/CVF conference on computer vision and pattern recognition*, 3186–3195.
- Zhao, H.; Jiang, L.; Jia, J.; Torr, P. H.; and Koltun, V. 2021. Point transformer. In *Proceedings of the IEEE/CVF International Conference on Computer Vision*, 16259–16268.
- Zheng, L.; Shen, L.; Tian, L.; Wang, S.; Wang, J.; and Tian, Q. 2015. Scalable person re-identification: A benchmark. In *Proceedings of the IEEE international conference on computer vision*, 1116–1124.
- Zheng, L.; Zhang, H.; Sun, S.; Chandraker, M.; Yang, Y.; and Tian, Q. 2017. Person re-identification in the wild. In *Proceedings of the IEEE Conference on Computer Vision and Pattern Recognition*, 1367–1376.
- Zheng, M.; Karanam, S.; Wu, Z.; and Radke, R. J. 2019. Re-identification with consistent attentive siamese networks. In *Proceedings of the IEEE/CVF Conference on Computer Vision and Pattern Recognition*, 5735–5744.
- Zheng, Z.; Zheng, L.; and Yang, Y. 2017. A discriminatively learned cnn embedding for person reidentification. *ACM transactions on multimedia computing, communications, and applications (TOMM)*, 14(1): 1–20.
- Zhong, Z.; Zheng, L.; Kang, G.; Li, S.; and Yang, Y. 2020. Random erasing data augmentation. In *Proceedings of the AAAI conference on artificial intelligence*, volume 34, 13001–13008.
- Zhu, H.; Ke, W.; Li, D.; Liu, J.; Tian, L.; and Shan, Y. 2022. Dual Cross-Attention Learning for Fine-Grained Visual Categorization and Object Re-Identification. In *Proceedings of the IEEE/CVF Conference on Computer Vision and Pattern Recognition*, 4692–4702.
- Zhu, K.; Guo, H.; Liu, Z.; Tang, M.; and Wang, J. 2020. Identity-guided human semantic parsing for person re-identification. In *European Conference on Computer Vision*, 346–363. Springer.
- Zhu, K.; Guo, H.; Zhang, S.; Wang, Y.; Huang, G.; Qiao, H.; Liu, J.; Wang, J.; and Tang, M. 2021. AAformer: Auto-aligned transformer for person re-identification. *arXiv preprint arXiv:2104.00921*.